Different Relationships Between Spring SST in the Indian and Pacific Oceans and Summer Precipitation in China

LI Yi[1] (李　熠), WU Bingyi[2]* (武炳义), YANG Qiuming[1] (杨秋明), and HUANG Shicheng[1] (黄世成)

1 *Jiangsu Institute of Meteorological Sciences, Nanjing* 210008

2 *Chinese Academy of Meteorological Sciences, Beijing* 100081

ABSTRACT

Observational and reanalysis data are used to investigate the different relationships between boreal spring sea surface temperature (SST) in the Indian and Pacific oceans and summer precipitation in China. Partial correlation analysis reveals that the effects of spring Indian Ocean SST (IO SST) and Pacific SST (PSST) anomalies on summer precipitation in China are qualitatively opposite. When IO SST anomalies are considered independently of PSST anomalies, precipitation decreases south of the Yangtze River, in most areas of Inner Mongolia, and in some parts of Liaoning Province, and increases in the Yangtze River valley, parts of southwestern and northern China, northeastern Inner Mongolia, and Heilongjiang Province. This results in a negative-positive-negative-positive pattern of precipitation anomalies in China from south to north. When PSST anomalies (particularly those in the Niño3.4 region) are considered independently of IO SST anomalies, the pattern of precipitation anomalies in China is positive-negative-positive-negative from south to north. The genesis of summer precipitation anomalies in China is also examined when El Niño–Southern Oscillation (ENSO) signals are removed from the ocean and atmosphere. An anticyclonic low-level wind anomaly forms in the South China Sea-Northwest Pacific area when the IO SST anomaly (SSTA) is warm and the Northwest Pacific SSTA is cold. This anticyclonic anomaly substantially influences summer precipitation in China. Anomalous warming of tropical IO SST induces positive geopotential height anomalies in the subtropics and an east-west dipole pattern in midlatitudes over Asia. These anomalies also affect summer precipitation in China.

Key words: Indian Ocean, Pacific Ocean, SST, summer precipitation

Citation: Li Yi, Wu Bingyi, Yang Qiuming, et al., 2013: Different relationships between spring SST in the Indian and Pacific oceans and summer precipitation in China. *Acta Meteor. Sinica*, **27**(4), 509–520, doi: 10.1007/s13351-013-0501-4.

1. Introduction

The world's oceans are one of the most important factors in determining atmospheric anomalies. The ocean varies much more slowly than the atmosphere, with a strong "memory" that results in a sustained effect on the atmosphere. Many previous studies have examined the influences of sea surface temperature (SST) in the eastern equatorial Pacific, the western Pacific warm pool, and the Indian Ocean (IO) on summer precipitation in China. As a strong signal on the interannual timescale in the tropical Pacific air-sea system, the El Niño-Southern Oscillation (ENSO) is a strong source of interannual variability

in the tropical Pacific air-sea system that significantly influences weather and climate anomalies both globally (Webster et al., 1998) and within China (Yu and Jiang, 1994). The impact of ENSO on precipitation in China has been one of the main concerns of Chinese scientists. Huang and Wu (1989) reported that summer monsoon precipitation increased in the Yangtze-Huaihe River valley but decreased in northern China and south of the Yangtze River during the El Niño developing stage. By contrast, precipitation anomalies were opposite during the El Niño decaying stage. Jin and Tao (1999) also found that different phases of ENSO had different impacts on summer precipitation in eastern China. Zhang et al. (1996) showed that

the impact of El Niño on precipitation in southern China resulted from the development of an abnormal atmospheric circulation over East Asia during the mature stage of El Niño, with different impacts by season (Zhang et al., 1999, Zhang and Sumi, 2002). Wu et al. (2003) identified two main seasonal rainfall anomalies in East Asia induced by the anomalous circulation systems associated with different phases of ENSO. Long and Li (1999) simulated below-average precipitation in eastern China during the summer following an El Niño event and below-average precipitation in the Yangtze-Huaihe River valley during the summer following a La Niña event. ENSO is therefore often used as an important predictor of summer precipitation in China. However, Gao and Wang (2007) pointed out that the significance of ENSO as a predictor of summer precipitation in China has declined since the 1970s. Some preliminary studies have also shown that ENSO-related precipitation anomaly patterns in China were opposite before and after the mid 1970s (Gao, 2006; Zhang et al., 2008). Ashok et al. (2007) identified a decrease in the frequency of ENSO events in recent years that has resulted in changes in the ENSO influence on traditional regions. These results suggest that more attention should be paid to how SST changes in other ocean basins influence summer precipitation in China.

Saji et al. (1999) introduced the concept of the Indian Ocean Dipole (IOD). Subsequent studies have raised questions regarding whether the IOD is a local air-sea coupling phenomenon independent of the Pacific (Behera et al., 1999; Webster et al., 1999; Yamagata et al., 2002; Yu and Lau, 2005), or whether it has a strong relationship with ENSO (Murtugudde et al., 2000; Xie et al., 2002; Baquero-Bernal et al., 2002; Krishnamurthy and Kirtman, 2003). Studies of the influence of IO SST on precipitation have focused on the relationship between the IOD and precipitation (Xiao et al., 2002); however, Xie et al. (2009), Yoo et al. (2006), and Yang et al. (2010) have found that the main mode of the IO SST anomaly (SSTA) was uniform temperature increase or decrease throughout the entire basin, and these uniform temperature changes are significantly correlated with ENSO and have a substantial influence on Asian monsoon climate. Wu et al.

(2009) demonstrated the importance of basin-wide Indian Ocean warming to the East Asian-western Pacific summer monsoon, and showed that it plays an active role in modifying the northwestern Pacific anomalous anticyclone during ENSO decay through atmospheric Kelvin waves and the Hadley circulation.

Recent studies have indicated that the Indian Ocean has a significant impact on climate variability during summer in the northwestern Pacific and East Asia (Yoo et al., 2006). Observations and model simulations show that the Indian Ocean plays a particularly important role in modifying the wind field over the western Pacific (Zhang and Yang, 2007; Zhang et al., 2009; Yoo et al., 2010; Kug and Kang, 2006). Xie et al. (2009) found that a warm IO SSTA could induce eastward-propagating warm equatorial Kelvin waves in the troposphere, while cold IO SSTA might induce cold equatorial Kelvin waves. These waves significantly affect the atmospheric circulation and summer climate anomalies over the northwestern Pacific and East Asia. Zhu and Houghton (1996) found that variability in the Asian summer monsoon is very sensitive to SST conditions in the tropical South Indian Ocean. Yu et al. (2003) showed that the Indian Ocean was more influential than the Pacific in determining the variability of tropical and monsoon climates during spring in an air-sea coupled model. The impact of IO SST on summer precipitation in China is therefore deserving a further study. Unlike the IOD, few studies have examined the influence of basin-wide changes in IO SST on summer precipitation in China. Likewise, although many previous studies have focused on ENSO, few have discussed the relative roles of the Pacific and Indian oceans. Wu et al. (2010) used numerical experiments to demonstrate that the relative contributions of SSTA in the tropical Indian Ocean and western Pacific to maintaining the northwestern Pacific anomalous anticyclone are seasonally dependent during El Niño decay. The contribution of local SSTA in the western Pacific occurred in early summer in their simulations, while that in the tropical Indian Ocean occurred in late summer. However, these results may be model-dependent. The present study therefore aims to determine a means of effectively se-

parating the role of SSTA in these two ocean basins using observational data. These results will then be used to determine the relative influences of IO SSTA and ENSO on summer precipitation in China.

2. Data and methods

The data used in the present study include: (1) monthly mean precipitation data from 160 stations over China compiled by the National Climate Center; (2) gridded ($2° \times 2°$) monthly SST data obtained from the National Oceanic and Atmospheric Administration (NOAA) Extended Reconstructed SST V3 (ERSST) dataset (Smith et al., 2008; Xue et al., 2003) (ftp://ftp.ncdc.noaa.gov/pub/data/cmb/ersst/v3b); and (3) gridded ($2.5° \times 2.5°$) atmospheric reanalyses of 500-hPa geopotential height and 850-hPa winds (u, v) obtained from NCEP/NCAR (Kalnay et al., 1996) (http://www.esrl.noaa.gov/psd/data/gridded/data.ncep.reanalysis.html). All three datasets are analyzed for the same period (1979–2010). Two analysis domains representing the Pacific (30°S–30°N, 110°E–80°W) and the Indian Ocean (30°S–30°N, 40°–115°E) are selected for this study.

The methods applied in this study include empirical orthogonal function (EOF) analysis, singular value decomposition (SVD), partial correlation analysis, and linear regression. EOF analysis is used to investigate the temporal and spatial variations of SSTA in the Pacific and Indian oceans during boreal spring. SVD is used to study the distributions of SSTA and summer precipitation in China, as well as the relationship between them. The partial correlation method is used to determine the differing impacts of IO SST and Pacific SST (PSST) anomalies on summer precipitation in China. Linear regression is used to remove ENSO signals from SST and atmospheric fields to more clearly identify the influence of SSTA on precipitation anomalies in China.

3. Dominant modes of variability in spring PSST and IO SST

Previous studies have commonly performed independent EOF analysis over either the Pacific or the Indian Ocean. In the present study, the EOF analysis is performed over both oceans as a combination (Fig. 1). The first EOF mode (Fig. 1a) contributes 35.55% of the total variance. Positive SSTA is apparent in the eastern equatorial Pacific, similar to the characteristic El Niño pattern. El Niño events are typically decaying during boreal spring, so the amplitude of SSTA in spring is less significant than in autumn or winter. The SSTA in the Indian Ocean is also positive and consistent throughout the entire IO analysis domain. The second EOF mode (Fig. 1b) contributes 18.8% of the total variance. This mode features negative SSTA in the eastern tropical Pacific, northwestern Pacific, and South Pacific, with positive SSTA in the eastern North Pacific. The IO SSTA is negative and consistent throughout the entire basin. The time coefficient of the first mode (Fig. 1c) varies mainly on interannual timescales, while the time coefficient of the second mode (Fig. 1d) varies on both interannual and interdecadal timescales. Both EOF patterns include consistent SST anomalies throughout the tropical Indian Ocean. The dominant modes of variability in the Indian Ocean must therefore be investigated separately.

Figure 2 shows the EOF analysis over the Indian Ocean. The first two EOF modes explain 43.59% and 14.05% of the total variance, respectively. The spatial distribution of the first mode (Fig. 2a) is very similar to the SSTA distribution in the Indian Ocean region shown in Fig. 1a. Variability in the corresponding time coefficient in Fig. 2c is again predominantly on interannual timescales. The correlation coefficient between the two time series in Figs. 1c and 2c is 0.43. The spatial distribution of the second mode (Fig. 2b) contains a clear east-west dipole, with positive SSTA in the east and negative SSTA in the west. The corresponding time coefficient (Fig. 2d) varies predominantly on interannual timescales, with no clear interdecadal variability. Both the spatial mode and the time coefficient differ substantially from those shown in Figs. 1b and 1d. The correlation coefficient between the two time series (Figs. 1d and 2d) is –0.19. An EOF analysis has also been performed for SSTA in the Pacific region (30°S–30°N, 110°E–80°W). The spatial distributions of the first two modes in the EOF
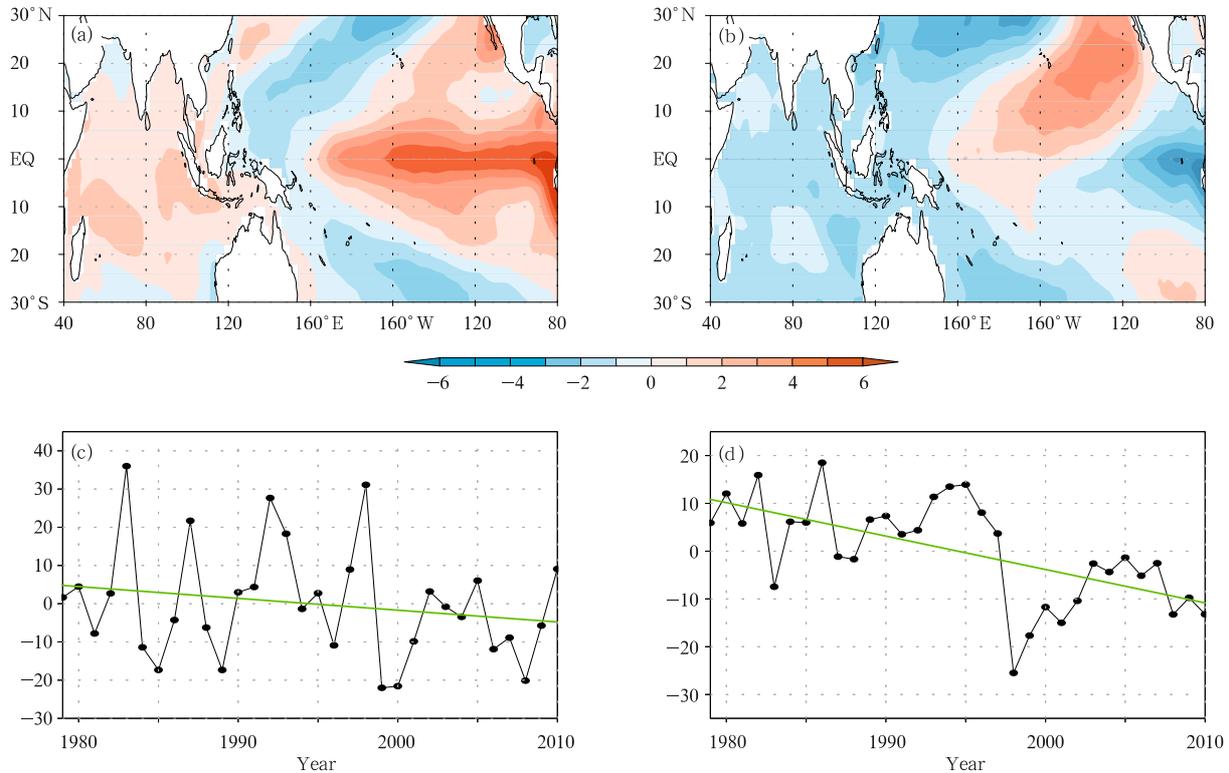
Fig. 1. (a, b) Spatial distributions and (c, d) time series of (a, c) EOF1 and (b, d) EOF2 of boreal spring SST anomalies in the Pacific–Indian Ocean.

analysis over the Pacific domain (figure omitted) are similar to those of the first two modes of the full domain, with correlation coefficients of 0.99 between the two time series in Figs. 1c and 2c and 0.96 between the two time series in Figs. 1d and 2d. Considering the two oceans as a unit primarily captures the variability in the Pacific while concealing the variability in the Indian Ocean. It is therefore necessary to investigate the Indian Ocean and its influence on precipitation in China independently.

The leading mode of PSST variability is consistent with that reported by other studies, while the second mode of IO SST variability is consistent with some but not all previous results. Many previous studies have identified close links between variations in IO SST and PSST (Yoo et al., 2010; Kug and Kang, 2006; Zhu and Houghton, 1996), but the correlation coefficient between the time series shown in Figs. 1c and 2c is only 0.43. This relatively low correlation suggests that IO SST also varies independently of PSST. The first EOF mode of the IO SSTA contains an approxi-

mately uniform basin-wide change in temperature regardless of whether the analysis is performed for the IO domain or the full domain. The atmospheric impact of this mode of variability in IO SST has not been studied as rigorously as the impact of the IOD.

4. Effects of boreal spring SSTAs in the Indian and Pacific oceans on summer precipitation in China

Interactions between the different ocean basins may cause anomalies in PSST to be implicitly contained in studies regarding relationships between IO SST and precipitation in China. Similarly, anomalies in IO SST may appear in studies regarding relationships between PSST and precipitation in China. Here, the independent influence of each ocean basin on precipitation in China is investigated by removing the component of SST variability that is related to anomalies in the other basin.
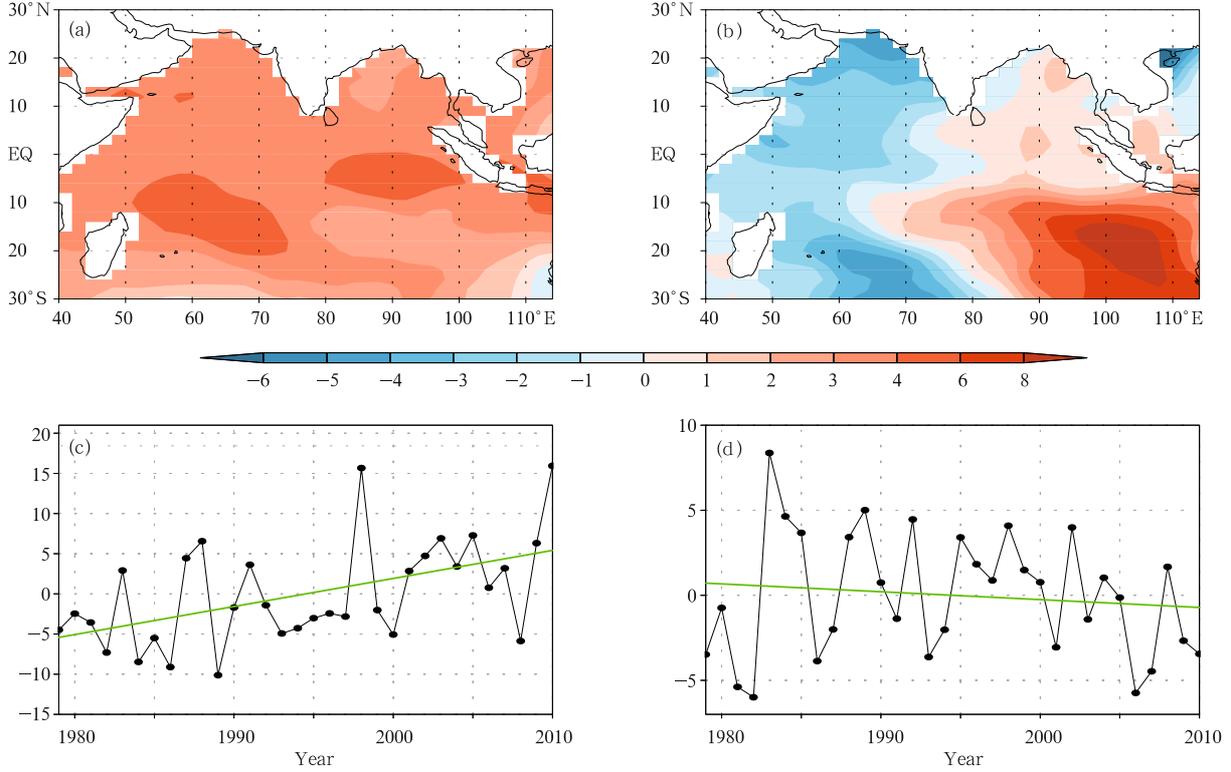
ENSO is the most significant mode of interannual

Fig. 2. (a, b) Spatial distributions and (c, d) time series of (a, c) EOF1 and (b, d) EOF2 of boreal spring SST anomalies in the Indian Ocean (30°S–30°N, 40°–115°E).

variability in PSST anomalies. The Niño3.4 index is therefore used to characterize SSTA in the Pacific. As this study focuses on the first EOF mode of the IO SSTA, the time series shown in Fig. 2c (abbreviated as IOidx) is used to characterize SSTA in the Indian Ocean. Figure 3 shows the Niño3.4 index (solid line) and the IOidx (dashed line) after removing the linear trends. The correlation coefficient between the two indices is 0.59. It should be emphasized that in this study PSSTA targets ENSO variability, while IO SSTA targets variations in the first EOF mode.

The influences of each ocean basin on precipitation in China are evaluated by applying the partial correlation method (Behera and Yamagata, 2003) to the indices shown in Fig. 3. Any SSTAs in the Indian Ocean that were linearly related to Niño3.4 are deducted from the IO SST. Likewise, any SSTAs in the Pacific Ocean that were linearly related to IOidx are deducted from PSST. This procedure enables an investigation of how variability in PSST and IO SST independently influences precipitation in China. The

partial correlation equation is defined as

$$
\begin{aligned}
r_{\mathrm{IP,N}} &= (r_{\mathrm{IP}} - r_{\mathrm{IN}}r_{\mathrm{NP}})/\sqrt{(1 - r_{\mathrm{NP}}^2)(1 - r_{\mathrm{IN}}^2)}, \\
r_{\mathrm{NP,I}} &= (r_{\mathrm{NP}} - r_{\mathrm{IN}}r_{\mathrm{IP}})/\sqrt{(1 - r_{\mathrm{IP}}^2)(1 - r_{\mathrm{IN}}^2)},
\end{aligned}
\tag{1}
$$

where $r_{\mathrm{IP,N}}$ represents the correlation coefficient between the boreal spring IOidx with Niño3.4 influences removed and the late summer precipitation anomaly over China, $r_{\mathrm{NP,I}}$ represents the correlation coefficient between the boreal spring Niño3.4 index with IOidx influences removed and the late summer precipitation anomaly over China, r_{IP} represents the correlation coefficient between the spring IOidx and the late summer precipitation anomaly, r_{IN} represents the correlation coefficient between the spring IOidx and the spring Niño3.4 index, and r_{NP} represents the correlation coefficient between the spring Niño3.4 index and the late summer precipitation anomaly. Statistical significance is evaluated using the two-tailed t-test.

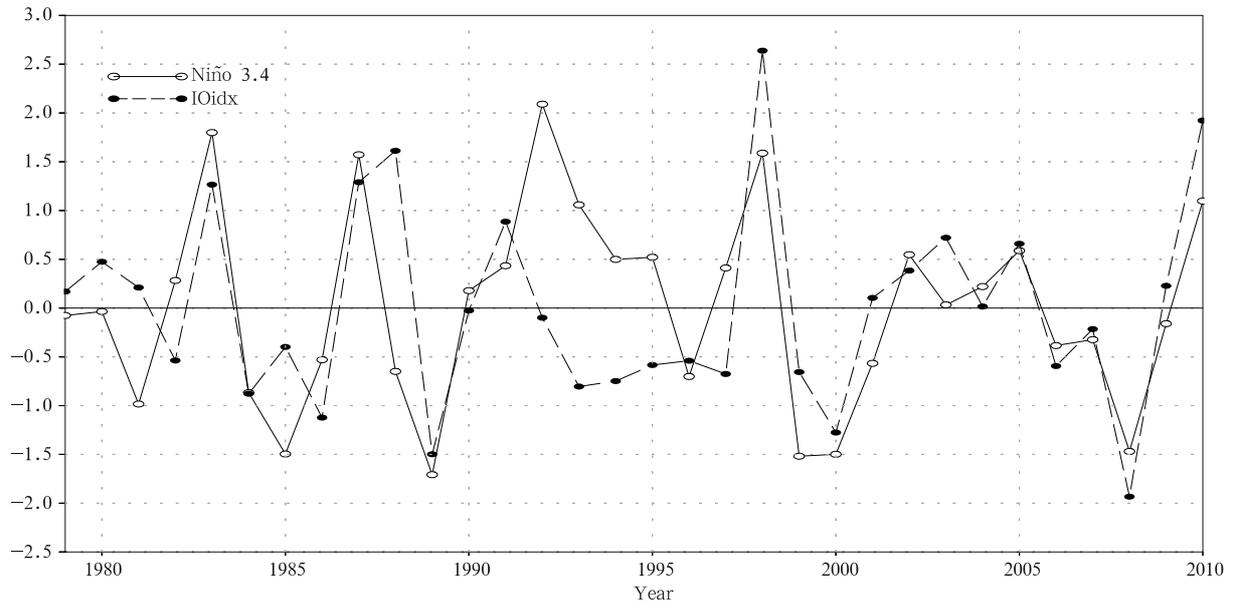Figure 4 shows the results of the partial correlation analysis between the boreal spring IOidx/Niño3.4

Fig. 3. Normalized and detrended Niño3.4 (solid line) and IOidx (dashed line) indices during boreal spring.
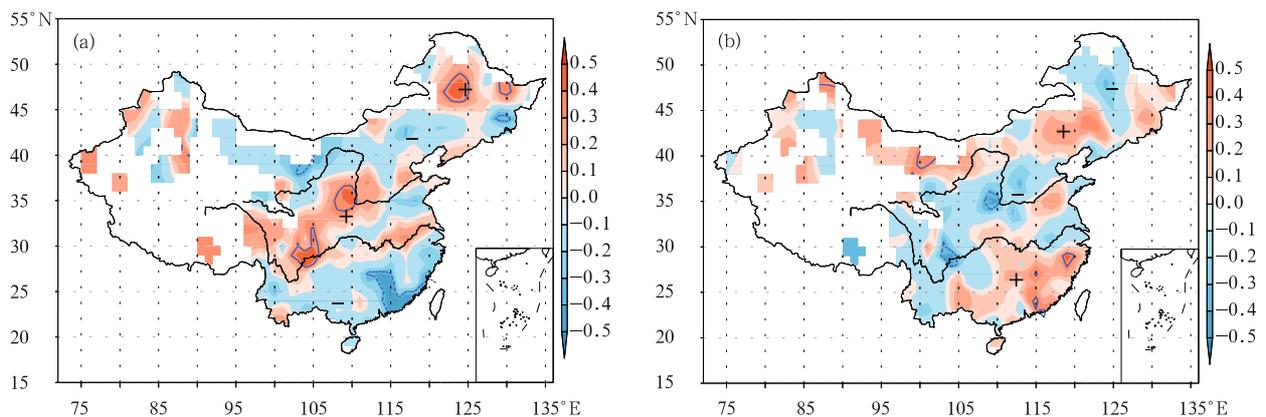

Fig. 4. Partial correlation maps between anomalous precipitation during late summer in China and (a) spring IOidx and (b) Niño3.4 index. Blue contours represent precipitation anomalies that are significant at the 95% confidence level.

and summer precipitation in China. A positive IOidx anomaly may reduce precipitation in the area south of the Yangtze River, most of Inner Mongolia, and parts of Liaoning Province (Fig. 4a). Conversely, a positive IOidx anomaly may enhance precipitation in the Yangtze River valley, southwestern and northern China, northeastern Inner Mongolia, and parts of Heilongjiang Province. A positive Niño3.4 index appears to have the opposite effect on precipitation in China (Fig. 4b). These results indicate that changes induced by spring IO SSTA may counteract changes induced

by PSST anomalies (labeled as "+" and "–" in Fig. 4). Although the correlation coefficient between the IOidx and Niño3.4 index is 0.59, the ways in which these two ocean basins influence precipitation in China may differ.

5. Influences of spring SST on summer precipitation in China after removing the ENSO signal

The impact of ENSO on precipitation in China

has been studied widely. It is therefore valuable to consider the influence of SSTAs with the ENSO signal removed on precipitation in China. The ENSO signal is removed from the SST and precipitation fields using the linear regression method outlined by An (2003). The specific method is as follows.

The variable $\xi^*(x, y, t)$ is defined as a function of space (x, y) and time (t), while the time series $Z(t)$ (i.e., Niño3.4 index) is defined as a function of time t. The modified variable $\xi(x, y, t)$ is calculated by removing the signal of $Z(t)$ from $\xi^*(x, y, t)$:

$$\xi = \xi^* - Z \times \text{cov}(\xi^*, Z)/\text{var}(Z), \qquad (2)$$

where cov and var represent the time covariance and variance, respectively. Equation (2) ensures that the $\text{cov}(\xi, Z)$ is zero at every spatial location, so that ξ is independent of Z.

An SVD is performed on boreal spring SSTA and summer precipitation anomalies in China after removing the ENSO signal. The first two modes are shown in Fig. 5. The first and second modes contribute 34.6% and 15.4% of the total covariance, respectively, with corresponding hetero-correlation coefficients of 0.85 and 0.77. The main modes of SSTA variability in the Indian Ocean remain uniform basin-wide increases or decreases in temperature even after removal of the ENSO signal; however, the ENSO pattern is removed from the leading modes of SSTA variability in the eastern tropical Pacific (Figs. 5c and 5d). The corresponding spatial distributions of precipitation are significantly different from the first and second modes shown in Fig. 5. The first mode (Fig. 5a) is characterized by increases in summer precipitation over Mongolia, northeastern and northwestern China, and decreases over most other parts of China. The second mode (Fig. 5b) is characterized by decreases in precipitation over most regions south of the Yangtze River and increases in the Yangtze River valley, northern and northeastern China, and parts of Mongolia. The time series corresponding to the first mode (Fig. 5e) is similar to that over the full analysis domain (Fig. 1d), with clear interdecadal variations and an abrupt change around 1997. By contrast, the time series associated with the second mode (Fig. 5f) varies mainly

on interannual timescales. The time series based on SSTA (black solid lines in Fig. 5f) are similar to IOidx, with statistically significant ($> 99\%$) correlation coefficients as high as 0.6. This study primarily concerns variability on interannual timescales, so the following analysis will focus on the relationship between boreal spring SSTAs and anomalous summer precipitation in China shown in Figs. 5b and 5d. The relationship shown in Figs. 5a and 5c, which varies predominantly on interdecadal timescales, will be largely ignored, although it is worth noting that Fig. 5c suggests that the recent weakening of the East Asian summer monsoon may be attributable to warming in the tropical Indian and western Pacific oceans. This result is consistent with the conclusions of previous studies (Zhou et al., 2008, 2009).

In Figs. 5b and 5d, it is seen that uniform basin-wide warming in the Indian Ocean is associated with decreases in precipitation over most parts of the region south of the Yangtze River and increases in precipitation over the Yangtze River valley, northern and northeastern China, and parts of Mongolia. Figure 6 shows regression maps of anomalous summer precipitation relative to the detrended time series of boreal spring SSTA and vice versa. The regressed distributions of anomalous precipitation (Fig. 6a) and SSTA (Fig. 6b) are both similar to the anomalous distributions of precipitation and SSTA shown in Figs. 5b and 5d. For precipitation (Fig. 6a), this similarity extends not only to the spatial distribution but also to the center of the anomalies. The regressed SSTA is significant at the 95% confidence level for most of the Indian Ocean, but for only a small portion of the Pacific Ocean between 10°S and 10°N. These results indicate that IO SSTAs have a more substantial influence on precipitation over China than Pacific SSTAs when the ENSO signal is removed. The distribution of anomalous precipitation when ENSO signals are removed from SSTAs is consistent with the distribution of anomalous precipitation (Fig. 4a) associated with IO SSTAs. This further indicates that IO SSTAs dominate the non-ENSO relationship between anomalous SST and anomalous precipitation over China.
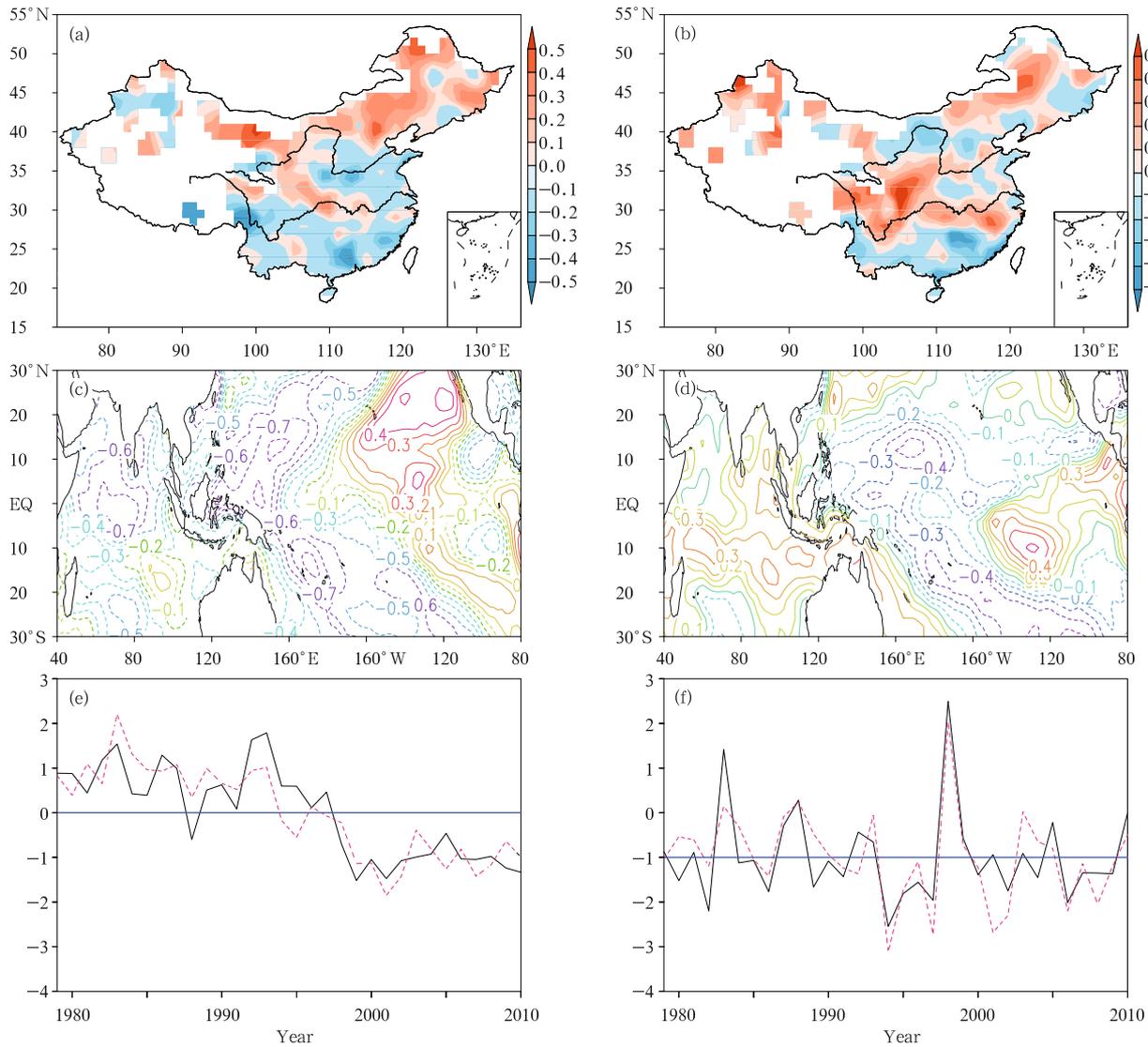
Fig. 5. Hetero-correlation fields for (a, b) precipitation, (c, d) SST, and (e, f) time series of (a, c, e) SVD1 and (b, d, f) SVD2 for Pacific-Indian Ocean SST anomalies during boreal spring and summer precipitation anomalies in China after removing the ENSO signal. The solid and dashed lines in (e, f) denote the SST and precipitation time series, respectively.

6. Analysis and discussion

This section explores possible mechanisms behind the impacts of boreal spring SSTA without ENSO signals (Fig. 5d) on anomalous summer precipitation over China. Figure 7 shows anomalous summer 500-hPa geopotential height and 850-hPa wind fields regressed against the detrended time series of SSTA without ENSO signals (solid line in Fig. 5f, and no trend). The regressed summer anomalous 500-hPa

geopotential height field in the Northern Hemisphere (Fig. 7a) contains a statistically significant positive anomaly in the region from the Philippine Islands to subtropical Indochina, including the region south of the Yangtze River. Moreover, an east-west dipole of geopotential height anomalies occurs over midlatitude Asia, with negative anomalies in the east and positive anomalies in the west, and a summer blocking anticyclone is apparent over the Sea of Okhotsk (located to the north of Japan). The regressed anomalous
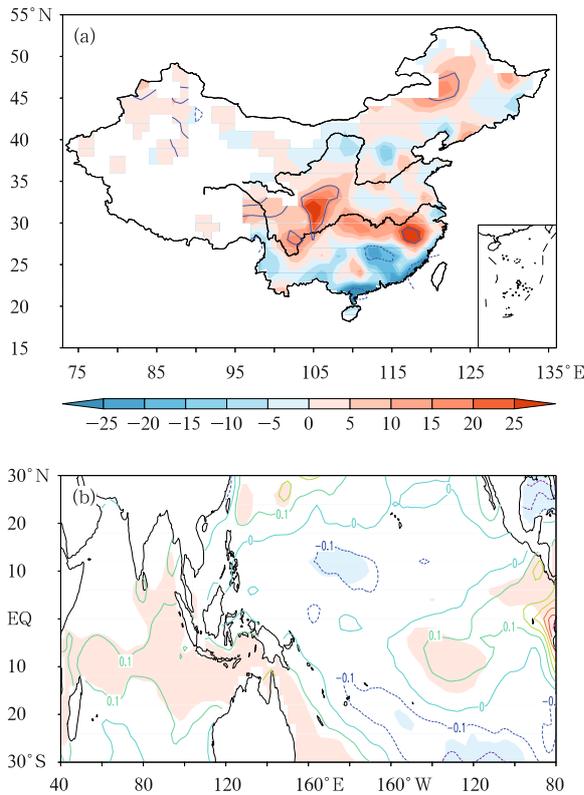
Fig. 6. (a) Regression map of summer precipitation anomalies (mm) against detrended SSTA (black solid line in Fig. 5f). Blue contours represent precipitation anomalies significant at the 95% confidence level. (b) Regression map of boreal spring SSTA (℃) against detrended precipitation anomalies (red dashed line in Fig. 5f). Shaded areas represent SST anomalies (℃) significant at the 95% confidence level.

850-hPa wind field (Fig. 7b) contains a significant easterly wind anomaly along the equator in the tropical western Pacific region and a prominent low-level anticyclone over the South China Sea and northwestern Pacific Ocean. This anomalous anticyclone shifts westward relative to the anticyclone reported by Wang et al. (2003) and extends partially over mainland China. A convergence belt in the 850-hPa wind field appears around 30°N, between the cyclonic anomalies north of 30°N and the anticyclonic anomaly south of 30°N. This convergence belt favors the formation of precipitation. A positive geopotential height anomaly prevails to the south of 30°N in the regressed 500-hPa geopotential height field, while a negative anomaly

prevails to the north (Fig. 7a). This is consistent with the positive precipitation anomaly near 30°N shown in Figs. 5b and 6a. Conversely, the positive 500-hPa geopotential height anomaly and anticyclonic circulation in the subtropics south of 30°N correspond to a negative precipitation anomaly (Figs. 5b and 6a).

The regressed SSTA field shown in Fig. 6b indicates that precipitation over China is strongly affected by SSTAs mainly in the Indian Ocean, particularly in the southern Bay of Bengal just north of the equator. Easterly anomalies in low-level wind near the equator are a part of the atmospheric response to positive SSTA in the tropical IO and the accompanying Kelvin wave (Gill, 1980). The most significant 500-hPa geopotential height response to heating of the tropical IO is located over the extratropical and midlatitude regions of continental Asia, consistent with the conclusions of Lin (2009). The summer blocking high near the Sea of Okhotsk may also influence summer precipitation in China (Wu and Zhang, 2011). The negative SSTA in Northwest Pacific (Fig. 6b) contributes to the formation of the anticyclonic anomaly over the South China Sea (Fig. 7b). The easterly wind anomalies in the tropics enhance this anticyclone. Positive tropical IO SSTA and negative northwestern PSST anomalies combine to induce a strong anticyclonic anomaly over the South China Sea-Northwest Pacific region. This anticyclonic anomaly exerts substantial influences on the climate over East Asia (Zhang et al., 1996). Lau and Nath (2000) showed that the Northwest Pacific anticyclone plays an important role in the East Asian summer monsoon system. Positive IO SSTAs related to ENSO promote the development and maintenance of this anticyclone during boreal summer through a mechanism similar to that of a thermal capacitor (Behera et al., 1999; Murtugudde et al., 2000). This study has shown that the development of an anticyclonic anomaly over the South China Sea-Northwest Pacific area is not dependent on ENSO; rather, this anomaly can arise independently from local negative SSTAs in Northwest Pacific and positive SSTAs in the tropical Indian Ocean. Wu et al. (2010) have previously demonstrated this result using idealized SSTA-driven AGCM experiments.
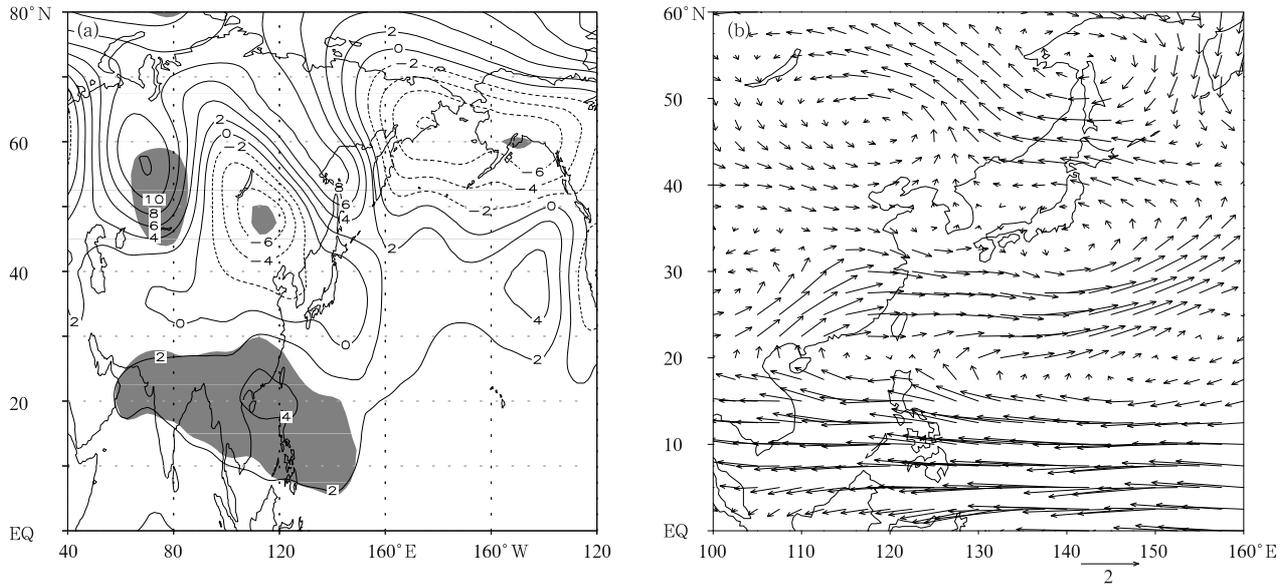
Fig. 7. Regression maps of summer (a) 500-hPa height anomalies (gpm) and (b) 850-hPa wind anomalies (m s^{-1}) against detrended SSTA (black solid line in Fig. 5f). Shaded areas in (a) represent values significance at the 95% confidence level.

They showed that the combined effects of local SSTAs in the tropical Indian Ocean and northwestern Pacific could create an anticyclonic anomaly in the western Pacific even in the absence of SSTAs in the equatorial central-eastern Pacific. Further study regarding the impact and extent of ENSO-related warming in the tropical IO and the formation of anticyclones in the western Pacific is still required.

7. Conclusions

The dominant modes of boreal spring variability in Pacific and Indian Ocean SST are derived, and the patterns of variability in IO SST are demonstrated to be more robust. Spring IO SST (with the portion related to the Niño3.4 index removed) and PSST (with the portion related to IO SST variability removed) are investigated and shown to have substantial influences on summer precipitation over China. Anomalous warming of the IO results in a negative-positive-negative-positive pattern of precipitation anomalies in eastern China from south to north. Anomalous warming in the Pacific region results in a qualitatively opposite distribution of precipitation anomalies. After removing ENSO signals, summer precipitation anomalies in China are influenced primarily by the

strength and position of the lower tropospheric anticyclone over the South China Sea–Northwest Pacific and related geopotential height anomalies in the middle troposphere. Positive SSTA in the IO induces remote atmospheric responses in the extratropical and midlatitude regions of Asia. Low latitude easterly wind anomalies triggered by IO SSTA enhance the anomalous anticyclonic circulation in the South China Sea–Northwest Pacific. Recent observations have indicated a weakening of the ENSO influence on summer precipitation over China. If this trend continues, relationships with spring SSTA in the tropical IO may become increasingly useful for forecasting summer precipitation in China.

REFERENCES

An, S. -I., 2003: Conditional maximum covariance analysis and its application to the tropical Indian Ocean SST and surface wind stress anomalies. *J. Climate*, **16**, 2932–2938.

Ashok, K., S. K. Behera, S. A. Rao, et al., 2007: El Niño Modoki and its possible teleconnection. *J. Geophys. Res.*, **112**, C11007.

Baquero-Bernal, A., M. Latif, and S. Legutke, 2002: On dipole like variability of sea surface temperature in the tropical Indian Ocean. *J. Climate*, **15**, 1358–1368.

Behera, S. K., S. Krishnan, and T. Yamagata, 1999: Unusual ocean-atmosphere conditions in the tropical Indian Ocean during 1994. *Geophys. Res. Lett.*, **26**, 3001–3004.

——, and T. Yamagata, 2003: Influence of the Indian Ocean dipole on the southern oscillation. *J. Meteor. Soc. Japan*, **81**(1), 169–177.

Gao Hui, 2006: Decadal variation of the relationship between summer precipitation along the Huaihe River valley and SST over the equatorial eastern Pacific. *J. Appl. Meteor. Sci.*, **17**(1), 1–9. (in Chinese)

—— and Wang Yongguang, 2007: On the weakening relationship between summer precipitation in China and ENSO. *Acta Meteor. Sinica*, **65**(1), 131–137. (in Chinese)

Gill, A. E., 1980: Some simple solutions for heat-induced tropical circulation. *Quart. J. Roy. Meteor. Soc.*, **106**, 447–462.

Huang Ronghui and Wu Yifang, 1989: The influence of ENSO on the summer climate change in China and its mechanism. *Adv. Atmos. Sci.*, **6**, 21–32.

Jin Zuhui and Tao Shiyan, 1999: A study on the relationships between ENSO cycle and rainfalls during summer and winter in eastern China. *Chinese J. Atmos. Sci.*, **23**(6), 663–672. (in Chinese)

Kalnay, E., M. Kanamitsu, R. Kistler, et al., 1996: The NCEP/NCAR 40-year reanalysis project. *Bull. Amer. Meteor. Soc.*, **77**, 437–471.

Krishnamurthy, V., and B. P. Kirtman, 2003: Variability of the Indian Ocean: Relation to monsoon and ENSO. *Quart. J. Roy. Meteor. Soc.*, **129**, 1623–1646.

Kug, J. S., and I. S. Kang, 2006: Interactive feedback between ENSO and the Indian Ocean. *J. Climate*, **19**, 1784–1801.

Lau, N. C., and M. J. Nath, 2000: Impact of ENSO on the variability of the Asian-Australian monsoons as simulated in GCM experiments. *J. Climate*, **13**, 4287–4309.

Lin Hai, 2009: Global extratropical response to diabatic heating variability of the Asian summer monsoon. *J. Atmos. Sci.*, **66**, 2697–2713.

Long Zhenxia and Li Chongyin, 1999: Numerical simulation of the ENSO influences on East Asian monsoon activities afterwards. *Acta Meteor. Sinica*, **57**(6), 651–661. (in Chinese)

Murtugudde, R., J. P. McCreary, and A. J. Busalacchi, 2000: Oceanic processes associated with anomalous events in the Indian Ocean with relevance to 1997–1998. *J. Geophys. Res.*, **105**, 3295–3306.

Saji, N. H., B. N. Goswami, P. N. Vinayachandran, et al., 1999: A dipole mode in the tropical Indian Ocean. *Nature*, **401**, 360–363.

Smith, T. M., R. W. Reynolds, T. C. Peterson, et al., 2008: Improvements to NOAA's historical merged land-ocean surface temperature analysis (1880–2006). *J. Climate*, **21**, 2283–2296.

Wang, B., R. G. Wu, and T. Li, 2003: Atmosphere-warm ocean interaction and its impacts on Asian-Australian monsoon variation. *J. Climate*, **16**, 1195–1211.

Webster, P. J., V. O. Magaña, T. N. Palmer, et al., 1998: Monsoons: Processes, predictability, and the prospects for prediction. *J. Geophys. Res.*, **103**, 14451–14510.

——, A. M. Moore, J. P. Loschnigg, et al., 1999: Coupled ocean-atmosphere dynamics in the Indian Ocean during 1997–98. *Nature*, **401**, 356–360.

Wu, B., T. J. Zhou, and T. Li, 2009: Seasonally evolving dominant interannual variability modes of East Asian climate. *J. Climate*, **22**, 2992–3005.

——, T. Li, and T. J. Zhou, 2010: Relative contributions of the Indian Ocean and local SST anomalies to the maintenance of the western North Pacific anomalous anticyclone during the El Niño decaying summer. *J. Climate*, **23**, 2974–2986.

Wu, R. G., Z. Z. Hu, and B. P. Kirtman, 2003: Evolution of ENSO-related rainfall anomalies in East Asia. *J. Climate*, **16**, 3742–3758.

Wu Bingyi and Zhang Renhe, 2011: Interannual variability of the East Asian summer monsoon and its association with the anomalous atmospheric circulation over the mid-high latitudes and external forcing. *Acta Meteor. Sinica*, **69**(2), 219–233. (in Chinese)

Xiao Ziniu, Yan Hongming, and Li Chongyin, 2002: Relationship between dipole oscillation of SSTA of Indian Ocean region and precipitation and temperature in China. *J. Trop. Meteor.*, **8**, 121–131.

Xie, S. P., H. Annamalai, F. A. Schott, et al., 2002: Structure and mechanisms of South Indian Ocean climate variability. *J. Climate*, **15**, 864–878.

——, K. M. Hu, J. Hafner, et al., 2009: Indian Ocean capacitor effect on Indo-western Pacific climate during the summer following El Niño. *J. Climate*, **22**, 730–747.

Xue, Y., T. M. Smith, and R. W. Reynolds, 2003: Interdecadal changes of 30-yr SST normals during 1871–2000. *J. Climate*, **16**, 1601–1612.

Yamagata, T., S. K. Behera, S. A. Rao, et al., 2002: The Indian Ocean dipole: A physical entity. *CLIVAR Exch.*, **24**(7), 2.

Yang Jianling, Liu Qinyu, and Liu Zhengyu, 2010: Linking observations of the Asian monsoon to the Indian Ocean SST: Possible roles of Indian Ocean basin mode and dipole mode. *J. Climate*, **23**, 5889–5902.

Yoo, S. H., S. Yang, and C. H. Ho, 2006: Variability of the Indian Ocean sea surface temperature and its impacts on Asian-Australian monsoon climate. *J. Geophys. Res.*, **111**, D03108.

——, J. Fasullo, S. Yang, et al., 2010: On the relationship between Indian Ocean sea surface temperature and the transition from El Niño to La Niña. *J. Geophys. Res.*, **115**, D15114.

Yu, J. Y., S. P. Weng, and J. D. Farrara, 2003: Ocean roles in the TBO transitions of the Indian-Australian monsoon system. *J. Climate*, **16**, 3072–3080.

——, and K. M. Lau, 2005: Contrasting Indian Ocean SST variability with and without ENSO influence: A coupled atmosphere-ocean GCM study. *Meteor. Atmos. Phys.*, **90**, 179–191.

Yu Zhihao and Jiang Quanrong, 1994: *El Niño, Anti-El Niño, and Southern Oscillation.* Nanjing University Press, Nanjing. 427 pp. (in Chinese)

Zhang, L., P. Chang, and M. K. Tippett, 2009: Linking the Pacific meridional mode to ENSO: Utilization of

a noise filter. *J. Climate*, **22**, 905–922.

Zhang, R. H., A. Sumi, and M. Kimoto., 1996: Impact of El Niño on the East Asian monsoon: A diagnostic study of the 86/87 and 91/92 events. *J. Meteor. Soc. Japan*, **74**, 49–62.

——, ——, and ——, 1999: A diagnostic study of the impact of El Niño on precipitation in China. *Adv. Atmos. Sci.*, **16**, 229–241.

——, and ——, 2002: Moisture circulation over East Asia during El Niño episode in northern winter, spring and autumn. *J. Meteor. Soc. Japan*, **80**, 213–227.

Zhang Qin and Yang Song, 2007: Seasonal phase-locking of peak events in the eastern Indian ocean. *Adv. Atmos. Sci.*, **24**, 781–798.

Zhang Renhe, Wu Bingyi, Zhao Ping, et al., 2008: The decadal shift of the summer climate in the late 1980s over eastern China and its possible causes. *Acta Meteor. Sinica*, **22**(4), 435–445.

Zhou, T. J., R. C. Yu, H. M. Li, et al., 2008: Ocean forcing to changes in global monsoon precipitation over the recent half-century. *J. Climate*, **21**, 3833–3852.

——, ——, J. Zhang, et al., 2009: Why the western Pacific subtropical high has extended westward since the late 1970s. *J. Climate*, **22**, 2199–2215.

Zhu, Y. L., and D. D. Houghton, 1996: The impact of Indian Ocean SST on the large-scale Asian summer monsoon and the hydrological cycle. *Int. J. Climatol.*, **16**, 617–632.